



HAL
open science

Empirical ugri-UBVRc transformations for galaxies

David O. Cook, Daniel A. Dale, Benjamin D. Johnson, Liese van Zee, Janice C. Lee, Robert C. Kennicutt, Daniela Calzetti, Shawn M. Staudaher, Charles W. Engelbracht

► **To cite this version:**

David O. Cook, Daniel A. Dale, Benjamin D. Johnson, Liese van Zee, Janice C. Lee, et al.. Empirical ugri-UBVRc transformations for galaxies. *Monthly Notices of the Royal Astronomical Society*, 2014, 445, pp.890-898. 10.1093/mnras/stu1581 . insu-03645247

HAL Id: insu-03645247

<https://insu.hal.science/insu-03645247>

Submitted on 25 Apr 2022

HAL is a multi-disciplinary open access archive for the deposit and dissemination of scientific research documents, whether they are published or not. The documents may come from teaching and research institutions in France or abroad, or from public or private research centers.

L'archive ouverte pluridisciplinaire **HAL**, est destinée au dépôt et à la diffusion de documents scientifiques de niveau recherche, publiés ou non, émanant des établissements d'enseignement et de recherche français ou étrangers, des laboratoires publics ou privés.

Empirical $ugri-UBVR_c$ transformations for galaxies

David O. Cook,^{1★} Daniel A. Dale,¹ Benjamin D. Johnson,² Liese Van Zee,³
Janice C. Lee,⁴ Robert C. Kennicutt,^{5,6} Daniela Calzetti,⁷
Shawn M. Staudaher¹ and Charles W. Engelbracht^{8†}

¹Department of Physics & Astronomy, University of Wyoming, Laramie, WY 82071, USA

²UPMC-CNRS, UMR7095, Institut d'Astrophysique de Paris, F-75014 Paris, France

³Department of Astronomy, Indiana University, Bloomington, IN 47405, USA

⁴Space Telescope Science Institute, 3700 San Martin Drive, Baltimore, MD 21218, USA

⁵Institute of Astronomy, University of Cambridge, Cambridge CB3 0HA, UK

⁶Steward Observatory, University of Arizona, Tucson, AZ 85721, USA

⁷Department of Astronomy, University of Massachusetts, Amherst, MA 01003, USA

⁸Raytheon Company, 1151 East Hermans Road, Tucson, AZ 85756, USA

Accepted 2014 July 31. Received 2014 July 29; in original form 2014 May 2

ABSTRACT

We present empirical colour transformations between Sloan Digital Sky Survey $ugri$ and Johnson–Cousins $UBVR_c$ photometry for nearby galaxies ($D < 11$ Mpc). We use the Local Volume Legacy (LVL) galaxy sample where there are 90 galaxies with overlapping observational coverage for these two filter sets. The LVL galaxy sample consists of normal, non-starbursting galaxies. We also examine how well the LVL galaxy colours are described by previous transformations derived from standard calibration stars and model-based galaxy templates. We find significant galaxy colour scatter around most of the previous transformation relationships. In addition, the previous transformations show systematic offsets between transformed and observed galaxy colours which are visible in observed colour–colour trends. The LVL-based *galaxy* transformations show no systematic colour offsets and reproduce the observed colour–colour galaxy trends.

Key words: galaxies: dwarf–galaxies: irregular–Local Group–galaxies: photometry–galaxies: spiral.

1 INTRODUCTION

The Sloan Digital Sky Survey (SDSS) is a large-area optical survey which covers more than one quarter of the sky (York et al. 2000). The five filters ($ugriz$) developed for this survey are based on a modified Thuan–Gunn (Thuan & Gunn 1976) system which provide wide optical wavelength coverage and little overlap between each filter bandpass. Due to the wide acceptance of this filter system, an increasing number of ground-based surveys utilize SDSS filters. Thus, there is a large amount of optical data for stars, galaxies, and quasars based on $ugriz$ photometry in addition to traditional $UBVR_cI_c$ photometry (Johnson & Morgan 1953; Cousins 1976).

All previous SDSS data releases have empirically characterized SDSS–Johnson–Cousins transformations for quasars (e.g. Jester et al. 2005) and stars (Pop I and II, metal-poor, dwarfs, and main sequence; Smith et al. 2002; Karaali, Bilir & Tunçel 2005; West,

Walkowicz & Hawley 2005; Jester et al. 2005; Jordi, Grebel & Ammon 2006; Rodgers et al. 2006). However, no study to date has explicitly investigated empirical transformations for a population of galaxies. It is reasonable to assume that some stellar transformations would describe galaxy transformations with relative accuracy since the majority of a galaxy's optical light emanates from stars. However, previous studies have found different transformations for stars with different metallicities (Karaali et al. 2005; Jordi et al. 2006) and different colours (Smith et al. 2002; Jester et al. 2005; West et al. 2005; Jordi et al. 2006). In addition, nebular emission and absorption are likely to significantly affect galaxy optical fluxes. It is not obvious if the transformations of stars with similar properties (i.e. metallicity and optical colour) would accurately describe a transformation of an amalgamation of stars with a wide range of properties (i.e. a galaxy) and account for nebular emission and absorption.

Although no previous study has investigated *empirical* galaxy transformations, the study of Blanton & Roweis (2007) has characterized transformations derived from model-based galaxy templates. These templates are a linear combination between observed galaxy

*E-mail: dcook12@uwyo.edu

†Deceased.

spectral energy distributions from large galaxy surveys (*GALEX*, SDSS, 2MASS, GOODS, DEEP2) and the stellar models of Bruzual & Charlot (2003). Although these transformations were derived for galaxies, they are dependent upon stellar models which introduce uncertainty based upon model assumptions (e.g. age, metallicity, initial mass function, stellar mass-to-light ratios) in addition to assumptions of a galaxy’s star formation history. It is not clear if transformations derived from model-based galaxy templates will accurately describe transformations for observed galaxy colours.

This study utilizes the Local Volume Legacy (LVL; Dale et al. 2009) survey galaxy sample to derive empirical SDSS–Johnson–Cousin transformations explicitly for galaxies. The LVL sample contains 90 galaxies with overlapping $UBVR_c$ and $ugriz$ observational coverage. This data set is ideal to characterize these transformations since the LVL sample consists of galaxies with a wide range of properties (e.g. morphology, metallicity, optical luminosity and colour, star formation rate, etc.). Furthermore, the sample is dominated by low-mass galaxies with low internal extinction (Dale et al. 2009; Cook et al. 2014b). These data in combination with previous stellar transformation relationships will facilitate an examination of how well stellar transformations describe galaxy transformations. In addition, we compare the LVL galaxy transformations to the Blanton & Roweis (2007) transformations derived from model-based galaxy templates.

2 SAMPLE

The LVL sample consists of 258 of our nearest galaxy neighbours reflecting a statistically complete, representative sample of the local Universe. The sample selection and description are detailed in Dale et al. (2009), but we provide an overview here.

The LVL sample was built upon the samples of two previous nearby galaxy surveys: ACS Nearby Galaxy Survey Treasury (Dalcanton et al. 2009) and 11 Mpc $H\alpha$ and Ultraviolet Galaxy Survey (11 HUGS; Kennicutt et al. 2008; Lee et al. 2011). The final LVL sample consists of galaxies that appear outside the Galactic plane ($|b| > 20^\circ$), have a distance less than 11 Mpc ($D \leq 11$ Mpc), span an absolute B -band magnitude of $-9.6 < M_B < -20.7$ mag, and span an RC3 catalogue galaxy type range of $-5 < T < 10$. Consequently, the LVL sample contains low-mass dwarf and irregular galaxies, large spirals, and a few elliptical galaxies.

There is significant $UBVR_c$ and $ugriz$ observational overlap. A total of 49, 85, 39, and 88 galaxies with $UBVR_c$ observations, respectively, also have $ugriz$ imaging available. Fig. 1 presents histograms of the full LVL sample (unshaded) and a subsample with overlapping $ugriz$ observational coverage (shaded). Both samples show relatively similar distributions of morphology, absolute B -band magnitude, star formation rate (SFR), and $B - R$ optical colour. The absolute B -band magnitudes and $B - R$ optical colours are taken from Cook et al. (2014a). The SFRs are derived from the *GALEX*

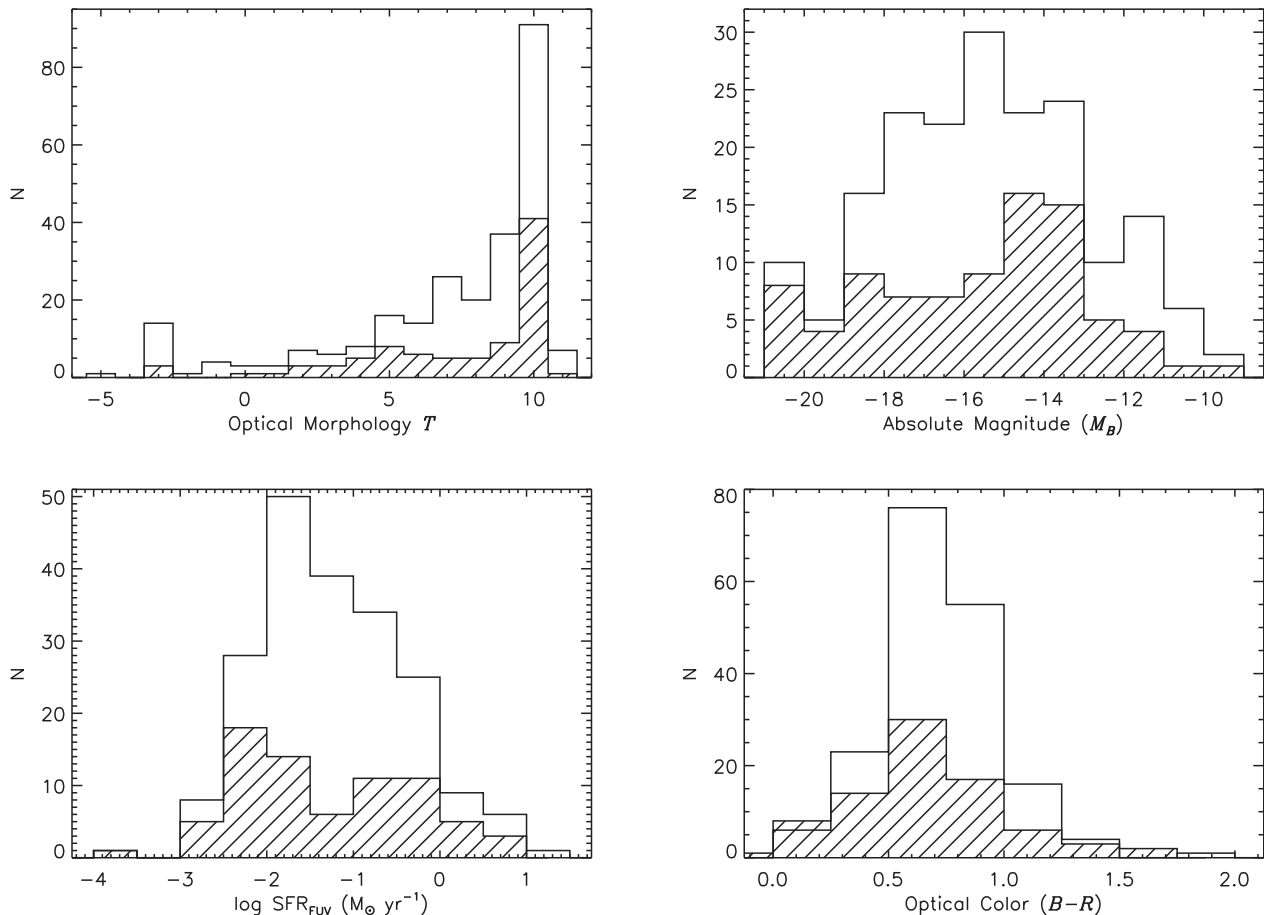


Figure 1. Distributions of RC3 morphology type taken from Kennicutt et al. (2008, top left), absolute B -band magnitude (top right), SFR (bottom left), and $(B - V)$ optical colour (bottom right). The unshaded histograms show the entire sample of 258 galaxies, whereas the shaded portions indicate a subsample of galaxies with overlapping $UBVR_c$ and $ugri$ observations.

far-ultraviolet magnitudes of Lee et al. (2011) and are transformed into SFRs via the prescription of Murphy et al. (2011).

3 DATA

We utilize the $UBVR_c$ and $ugri$ fluxes from the LVL global optical photometry study of Cook et al. (2014a). We do not use the z -band fluxes for our transformations since there are no corresponding I_c -band fluxes. These data are fully described in Cook et al. (2014a), but we provide a brief overview here.

The $UBVR_c$ ground-based data were taken from 1–2 m class telescopes. The images were reduced via standard IRAF tasks and the resulting photometry was calibrated to the Johnson–Cousins magnitude system via Landolt standard star observations taken several times a night. Since the fluxes of Cook et al. (2014a) are published in the AB magnitude system, we have recovered the Vega magnitudes via the prescription of Blanton & Roweis (2007).

The SDSS data were downloaded from SDSS DR7 (Abazajian et al. 2009). For each galaxy, mosaic images were constructed using the utility SWARP (Bertin et al. 2002), sky-subtracted, and photometrically calibrated to the AB magnitude system; note that the SDSS magnitudes are corrected for AB magnitude offsets as prescribed by the DR7 data release website.¹

To ensure accurate photometric comparisons across different optical bandpasses, Cook et al. (2014a) removed contaminating foreground stars and background galaxies from the optical images. Contaminant regions were overlaid on to each optical image, visually inspected, and the contaminant region sizes were adjusted to account for the relative apparent brightness of each source. Each contaminant was removed through an interpolation of the surrounding local sky using the IRAF task IMEDIT.

Global photometry is performed on both $UBVR_c$ and $ugri$ images within identical apertures defined by Dale et al. (2009). These apertures were chosen to encompass the majority of the emission seen at GALEX UV (1500–2300 Å) and Spitzer IR (3.6–160 μm) wavelengths, but we have visually checked to ensure that they are adequately large to encompass all of the optical emission of each galaxy. These apertures have a median semimajor axis ratio of 1.5 compared to R25 apertures (de Vaucouleurs et al. 1991).

4 RESULTS

In this section, we derive empirical colour transformations for galaxies using a subsample of LVL with overlapping $UBVR_c$ and $ugri$ imaging. We derive both $ugri$ -to- $UBVR_c$ and $UBVR_c$ -to- $ugri$ transformations and quantify the accuracy of all possible colour–colour combinations via the rms scatter and the resulting transformed minus observed magnitude for each colour transformation. We compare these results to previous transformations and examine how well all transformations reproduce observed colour–colour trends. The LVL galaxy transformations show better agreement with observed magnitudes and colours compared to previous transformations.

4.1 SDSS to Johnson–Cousins

In this section, we describe the methods used to derive the $ugri$ -to- $UBVR_c$ galaxy transformations. We quantify the accuracy of each transformation and compare them to previous transformations. In

addition, we perform a second accuracy check by comparing transformed colours to observed colour–colour trends.

4.1.1 LVL transformations for galaxies

To determine colour transformations between the SDSS and Johnson–Cousins magnitude systems, we examine all possible combinations of the difference in Johnson–Cousins and SDSS magnitudes versus SDSS colours (e.g. $U - r$ versus $g - r$). A least χ^2 fit is performed on each combination and the rms scatter about the best-fitting line is calculated. In addition, we calculate the median absolute difference between the transformed and observed magnitude (ΔM_{med}) for each colour transformation.

The combination of rms scatter and ΔM_{med} values together quantifies the accuracy of each colour transformation. A low rms scatter implies a well-behaved transformation (i.e. most galaxies show agreement with the best-fitting transformation). The ΔM_{med} values quantify how accurately the transformation (i.e. the best-fitting line to the data) reproduces the typical observed magnitudes for the sample.

The top panel of Fig. 2 shows ΔM_{med} versus the rms scatter of each LVL colour transformation. Above an rms value of ~ 0.12 mag, there exists a lower envelope in ΔM_{med} where the transformed magnitudes are increasingly inconsistent with the observed magnitude (i.e. higher ΔM_{med}). This trend suggests that transformations with low rms scatter should result in good agreement between transformed and observed magnitudes. However, there are a number of colour transformations with low rms scatter (< 0.12 mag) but relatively high ΔM_{med} values (> 0.05 mag). Thus, a combination of low rms scatter and low ΔM_{med} would provide the best available transformation for each filter. If we treat the rms scatter and ΔM_{med}

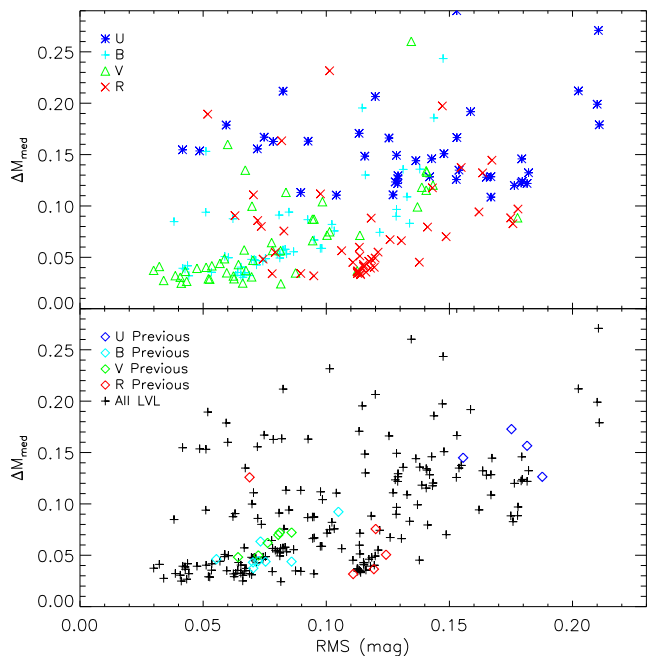


Figure 2. The median absolute difference between the transformed and observed magnitudes (ΔM_{med}) versus the rms scatter of each colour transformation. Top panel: all possible colour–colour transformation combinations of the LVL subsample with overlapping $UBVR_c$ and $ugri$ imaging. Bottom panel: transformations of previous studies derived from standard calibration stars overplotted on to the data of the top panel which are now presented as ‘plus’ signs.

¹ <http://www.sdss.org/dr7/algorithms/fluxcal.html>

Table 1. The *ugri*-to-*UBVR_c* transformation equations and coefficients for galaxies derived from a subsample of LVL where there exists an overlap between *UBVR_c* and *ugri* imaging. The last column lists the rms scatter of the LVL galaxy colours around the least χ^2 fit for each transformation.

SDSS transformations		
Colour	Colour transformation	rms (mag)
$U - i$	$= (1.93 \pm 0.06)(g - i) + (-0.48 \pm 0.04)$	0.09
$B - i$	$= (1.27 \pm 0.03)(g - i) + (0.16 \pm 0.01)$	0.04
$V - u$	$= (-0.82 \pm 0.03)(u - r) + (-0.02 \pm 0.04)$	0.03
$R - u$	$= (-1.06 \pm 0.02)(u - r) + (-0.11 \pm 0.03)$	0.08

values as a measure of each transformation’s uncertainty, we can add these quantities in quadrature, identify the lowest value as the transformation with the lowest uncertainty, and thus identify the best available transformation.

There are several *B*– and *V*-band transformations where both the rms scatter and ΔM_{med} values fall below 0.05 mag. Also, the *R_c*-band transformations show low ΔM_{med} values ($\Delta M_{\text{med}} < 0.05$) but slightly higher rms scatter ($0.05 < \text{rms} < 0.12$). For these three bandpasses (*BVR_c*), we choose the transformation with the lowest rms and ΔM_{med} values added in quadrature.

There are several *U*-band transformations which show low rms scatter (< 0.12 mag) but all show relatively high ΔM_{med} values (≥ 0.1 mag) compared to other bandpasses. The transformation with the lowest rms and ΔM_{med} value added in quadrature falls in Fig. 2 at an rms of ~ 0.09 and ΔM_{med} value of ~ 0.1 mag, respectively. The equations and best-fitting parameters of the *ugri*-to-*UBVR_c* LVL galaxy transformations are shown in Table 1. The individual LVL–colour transformation relationships are graphically presented in Fig. 3.

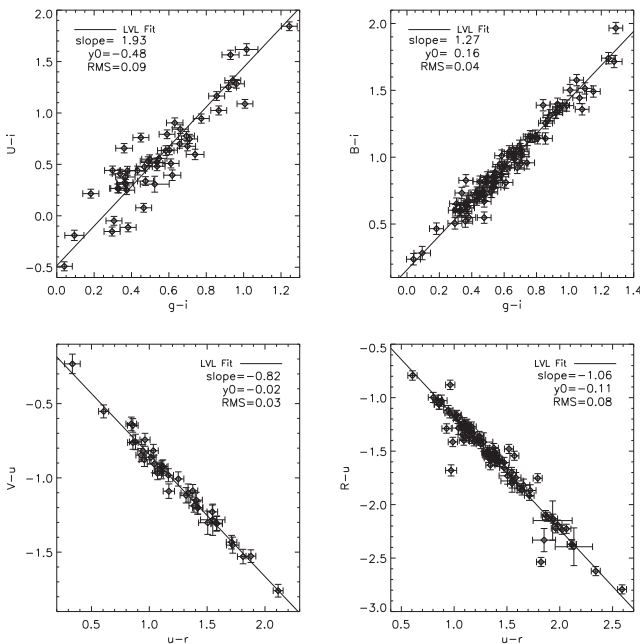


Figure 3. The colour–colour relationships used to define the LVL galaxy transformations. The solid black line is the least χ^2 fit to the galaxy colours and represents the LVL galaxy transformations. The fit parameters are listed in the caption as well as in Table 1.

4.1.2 Previous transformations

We also test how well the LVL galaxy colours are described by previous SDSS transformations. The studies of Jester et al. (2005), Jordi et al. (2006), and Blanton & Roweis (2007) derived *ugriz*-to-*UBVR_cI_c* transformations while Lupton’s (2005, hereafter L05)² transformations derived *ugriz*-to-*BVR_cI_c* transformations; there are no *U*-band transformations for L05. The studies of L05, Jester et al. (2005), and Jordi et al. (2006) utilized either Landolt standard stars (Landolt 1992) or an extension of Landolt’s standard stars (Stetson 2000) to derive stellar transformations, while Blanton & Roweis (2007) utilized model-based galaxy templates to derive galaxy transformations.

Fig. 4 graphically presents the colour transformation relationships of these previous studies with the LVL galaxy colours overlaid. Any previous transformation which utilizes *I*-band photometry has been omitted since the study of Cook et al. (2014a) did not publish such measurements. The LVL galaxy colours show a significant amount of scatter around most of these relationships and/or there exists an offset between the LVL-derived best fit and those derived from standard stars and model-based galaxy templates.

We calculate the rms scatter of the LVL galaxy colours around the previously published best-fitting lines and the ΔM_{med} values to quantify the accuracy of the previous transformations on galaxy colours. The results are graphically shown in the bottom panel of Fig. 2. The previous transformations show a similar trend across *UBVR_c* filters to those of LVL where the transformations of both the *B* and *V* bands show low rms scatter and ΔM_{med} values, that of the *R_c* band shows higher rms scatter but low ΔM_{med} values, and that of the *U* band shows relatively high rms scatter and ΔM_{med} values.

Although some of the *B*-, *V*-, and *R_c*-band transformations of previous studies provide reasonably low ΔM_{med} values, most of the corresponding colour–colour relationships show poor fits to observed galaxy colours. In addition, Fig. 2 shows that for every transformation derived in previous studies, there exists an LVL transformation with a lower rms scatter and ΔM_{med} value in every bandpass. Furthermore, the *U*-band transformations provide the highest contrast between the accuracies of the LVL and previous transformations. There are many LVL *U*-band transformations which are significantly lower in both rms scatter and ΔM_{med} values compared to the best *U*-band transformation derived from previous studies.

4.1.3 Observed Colour–colour trends

The rms scatter and ΔM_{med} values provide one way to quantify the accuracy of each transformation. Another means to test the accuracy of colour transformations is to propagate the transformed magnitudes into colours and examine how well these transformed colours reproduce observed colour–colour trends.

In general, galaxies show correlations between different optical colours with varying amounts of scatter (e.g. Blanton et al. 2003; Cook et al. 2014a). This scatter is reduced when the flux within each bandpass is corrected for internal extinction due to dust (Cook et al. 2014b). To test how well the LVL and previous transformations reproduce observed colour–colour relationships, we correct both the transformed and observed LVL galaxy fluxes for extinction due to dust.

² <https://www.sdss3.org/dr10/algorithms/sdssUBVRITransform.php>

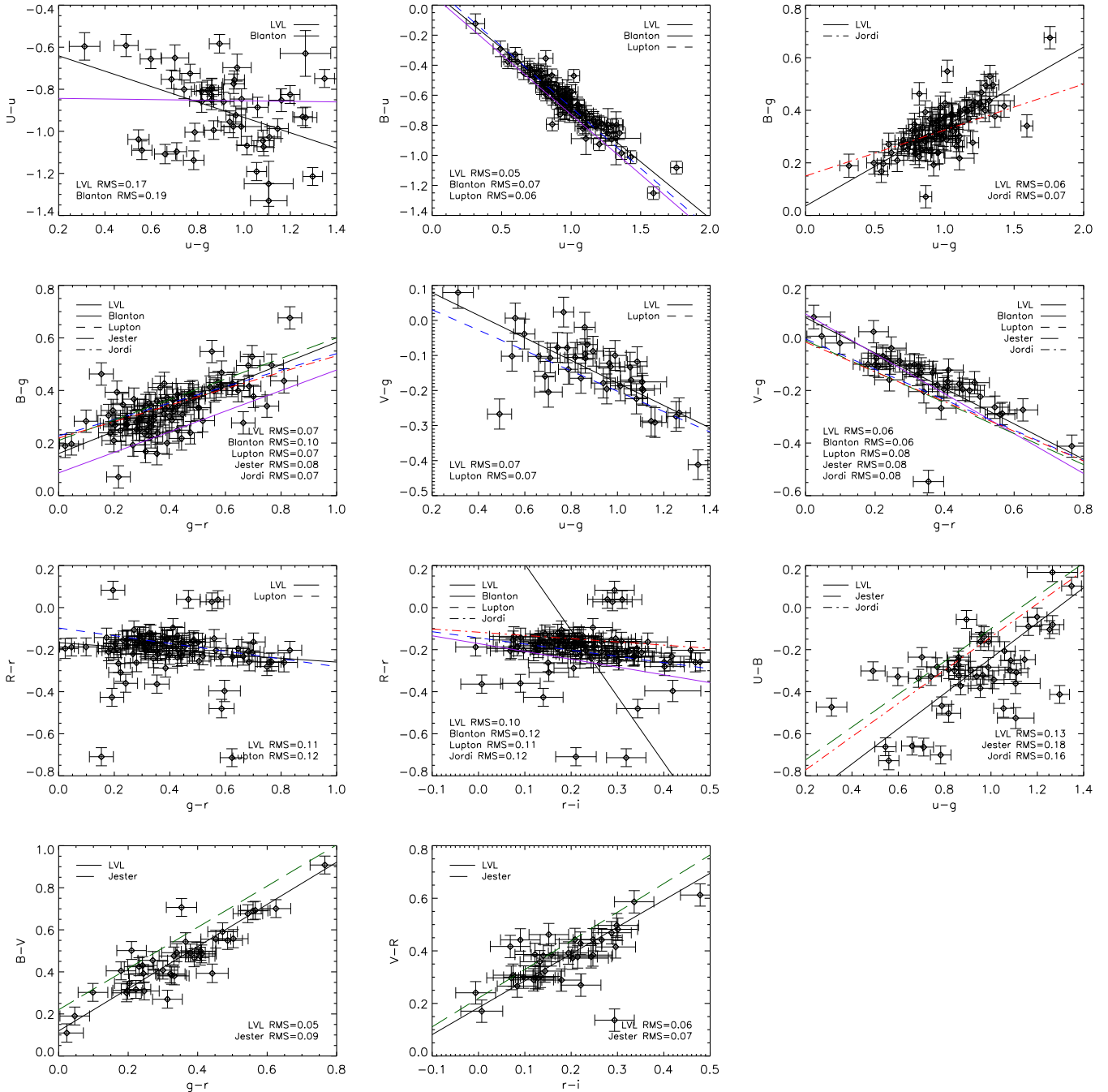


Figure 4. The colour–colour relationships used to derive the previous transformations of Jester et al. (2005), L05, Jordi et al. (2006), and Blanton & Roweis (2007). The open diamonds represent the observed LVL galaxy colours and the black solid line represents the best-fitting line to the data. The dashed, long-dashed, dash–dotted, and triple-dot–dashed lines represent the best-fitting lines published by the studies of Jester et al. (2005), L05, Jordi et al. (2006), and Blanton & Roweis (2007), respectively. Most panels show significant galaxy scatter or an offset between the LVL and stellar transformation best-fitting line.

The extinction corrections in each optical bandpass are carried out by Cook et al. (2014b) and are fully described there. Note that correcting for internal dust extinction does not change the difference between transformed and observed colours, but visually highlights any differences in colour–colour trends which are consequently tighter due to dust corrections. Quantities in this study which have been corrected for internal extinction due to dust are denoted with a subscript ‘0’ and represent an intrinsic measurement.

Figs 5 and 6 show two colour–colour relationships, where the observed $UBVR_c$ colours show relatively tight correlations with each other. The panels of Figs 5 and 6 present the observed-only colour–colour trend for a visual reference and subsequent comparison panels between observed and transformed colours. These comparison panels show colours transformed via the prescriptions of L05, Jester et al. (2005), Jordi et al. (2006), Blanton & Roweis (2007), and the LVL galaxy prescriptions presented in Table 1. When multiple

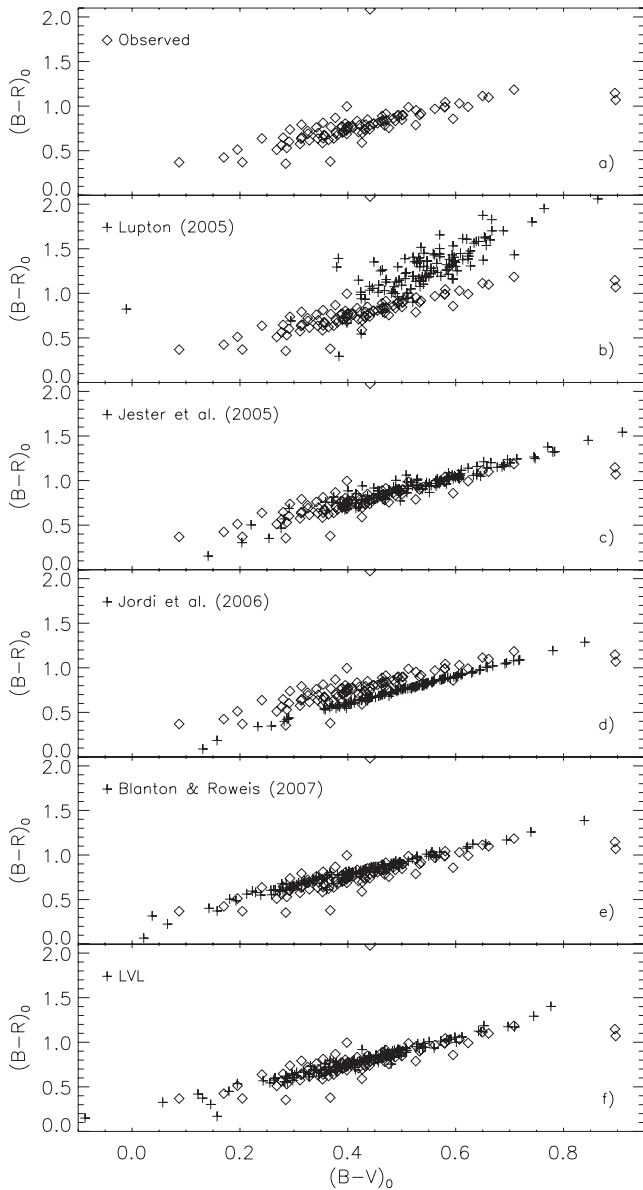


Figure 5. The colour–colour relationship between $(B - R)_0$ and $(B - V)_0$ where the flux of each bandpass in both colours has been corrected for internal extinction due to dust and Milky Way foreground extinction. Panel (a) is the observed trend with no transformed colours overplotted, panel (b) has the transformed colours via the prescription of L05 overplotted, panel (c) has the transformed colours via the prescription of Jester et al. (2005) overplotted, panel (d) has the transformed colours via the prescription of Jordi et al. (2006) overplotted, panel (e) has the transformed colours via the prescription of Blanton & Roweis (2007) overplotted, and panel (f) has the LVL transformed colours overplotted. Each of the stellar transformed colours shows colour offsets in both axes. These offsets are quantified in Table 2. The LVL transformed colours show good agreement with the observed colour trend.

previous transformations exist for a given bandpass, we choose the one which yielded the lowest ΔM_{med} value in the bottom panel of Fig. 2.

Fig. 5 shows the $(B - V)_0$ versus $(B - R)_0$ relationship where panel (a) is the observed trend with no transformed colours overplotted, panel (b) has the transformed colours via the prescription of L05 overplotted, panel (c) has the transformed colours via the prescription of Jester et al. (2005) overplotted, panel (d) has the

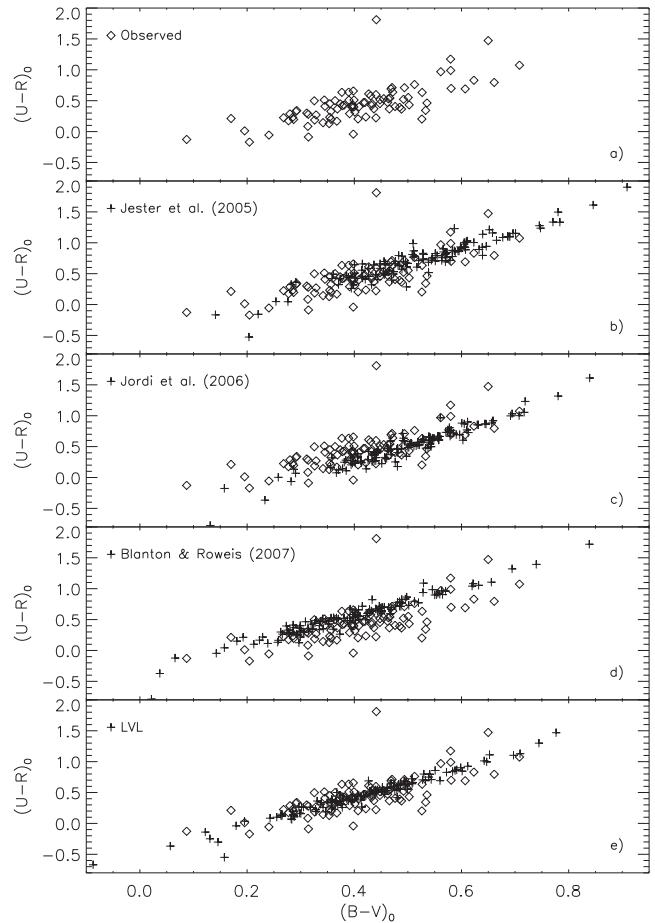


Figure 6. The colour–colour relationship between $(U - R)_0$ and $(B - V)_0$. Panel (a) is the observed trend with no transformed colours overplotted, panel (b) has the transformed colours via the prescription of Jester et al. (2005) overplotted, panel (c) has the transformed colours via the prescription of Jordi et al. (2006) overplotted, panel (d) has the transformed colours via the prescription of Blanton & Roweis (2007) overplotted, and panel (e) has the LVL transformed colours overplotted. Each of the stellar transformed colours shows colour offsets in both axes. These offsets are quantified in Table 2. The LVL transformed colours show good agreement with the observed colour trend.

transformed colours via the prescription of Jordi et al. (2006) overplotted, panel (e) has the transformed colours via the prescription of Blanton & Roweis (2007) overplotted, and panel (f) has the LVL transformed colours overplotted.

Visual inspection of Fig. 5 shows significant disagreement between the observed colour–colour trend and the transformed colours of L05 in both slope and colour offset. The transformed colours of Jester et al. (2005), Jordi et al. (2006), and Blanton & Roweis (2007) show similar slopes to that of the observed trend, but the Jordi et al. (2006) transformations show a noticeable offset.

Although the transformed colours of Jester et al. (2005) show a similar slope to that of the observed colours, there is an offset which is less obvious at first glance. Table 2 shows the median colour difference between the transformed and observed colours for the LVL and previous transformations. The median $\Delta(B - R)_0$ and $\Delta(B - V)_0$ colour differences for Jester et al. (2005) show that both colours are redder by 0.16 and 0.1 mag, respectively. The ratio of $\Delta(B - R)_0$ to $\Delta(B - V)_0$ represents the slope at which the Jester et al. (2005) colours are shifted and is similar to the slope of

Table 2. The median colour differences between the *ugri*-to-*UBVR_c* transformed and observed colours for the LVL galaxy transformations and those derived in previous transformations. The flux of each bandpass for all colours has been corrected for internal extinction due to dust.

Median colour differences		
Colour	Study	Δcolour (mag)
$(U - B)_0$	Jester et al. (2005)	0.15
	Jordi et al. (2006)	0.11
	Blanton & Roweis (2007)	0.13
	LVL	0.04
$(U - V)_0$	Jester et al. (2005)	0.29
	Jordi et al. (2006)	0.23
	Blanton & Roweis (2007)	0.14
	LVL	0.06
$(U - R)_0$	Jester et al. (2005)	0.24
	Jordi et al. (2006)	0.02
	Blanton & Roweis (2007)	0.06
	LVL	-0.01
$(B - V)_0$	Jester et al. (2005)	0.10
	Lupton (2005)	0.13
	Jordi et al. (2006)	0.08
	Blanton & Roweis (2007)	-0.03
	LVL	0.01
$(B - R)_0$	Jester et al. (2005)	0.16
	Lupton (2005)	0.50
	Jordi et al. (2006)	-0.01
	Blanton & Roweis (2007)	0.01
	LVL	0.01
$(V - R)_0$	Jester et al. (2005)	0.05
	Lupton (2005)	0.31
	Jordi et al. (2006)	-0.10
	Blanton & Roweis (2007)	0.03
	LVL	-0.01

the observed colour–colour trend (ratio of Δy to $\Delta x \sim 1.5$). Thus, the Jester et al. (2005) transformations show a similar $(B - R)_0$ and $(B - V)_0$ slope to that of the observed colours, but exhibit a systematic offset along the observed colour–colour relationship to redder colours (up and to the right in Fig. 5).

Both the LVL and Blanton & Roweis (2007) transformations show similar agreement between the transformed and observed colour slopes in Fig. 5, and show small colour offsets in Table 2. However, the LVL transformed colours consistently exhibit the lowest, or similar to the lowest, median colour differences in all colours, especially those which involve *U*-band transformations.

Fig. 6 shows another observed colour–colour trend where there exists a correlation between $(U - R)_0$ and $(B - V)_0$. Note that there is no L05 panel in Fig. 6 since there are no L05 *U*-band transformations.

Fig. 6 shows that the Jester et al. (2005), Jordi et al. (2006), and Blanton & Roweis (2007) transformations show a similar slope compared to the observed trend, but the transformed colours of both Jordi et al. (2006) and Blanton & Roweis (2007) show a noticeable offset. Inspection of Table 2 reveals that the Jester et al. (2005) transformations have redder median colours in both $(U - R)_0$ and $(B - V)_0$ similar to the observed colour–colour slope indicating a systematic offset along the observed colour–colour relationship. Furthermore, Table 2 shows that all previous transformations

exhibit greater median colour differences compared to the LVL transformations.

The LVL transformations show good agreement with the colour–colour trend in Fig. 6 and no systematic offset in the median colour differences in Table 2. In addition, only the LVL transformations show small median colour differences in colours which involve *U*-band transformations. Although *some* of the previous transformations show good agreement with *some* observed colour trends, only the LVL transformations show consistent agreement across all colours.

4.2 Johnson–Cousins to SDSS

In this section, we derive the *UBVR_c*-to-*ugri* galaxy transformations with identical methods to those described in Section 4.1. We verify the accuracy of these transformations and compare them to previous transformations via observed *ugri* colour–colour trends. However, we only present these results in tabular format since we observe similar trends to those found in Section 4.1.

4.2.1 LVL transformations for galaxies

We examine all possible combinations of SDSS minus Johnson–Cousins magnitudes versus Johnson–Cousins colours to derive the LVL galaxy transformations. The rms scatter and ΔM_{med} values are calculated for each transformation. The ΔM_{med} versus rms scatter plot for these transformations (not shown for brevity) has a similar overall structure to that of Fig. 2. There are multiple *ugri*-band transformations with low rms scatter and ΔM_{med} values (< 0.1 mag). For these bandpasses (*ugri*), we choose the transformations with the lowest rms and ΔM_{med} added in quadrature (see Section 4.1.1). There are no *z*-band transformations derived in this study due a lack of corresponding *I_c*-band fluxes. The *UBVR_c*-to-*ugri* galaxy transformation equations and best-fitting parameters are presented in Table 3.

4.2.2 Previous transformations

We also compare the LVL *UBVR_c*-to-*ugri* galaxy transformations to those of previous studies. However, the study of L05 does not provide Johnson–Cousins-to-SDSS transformations; thus, there are no comparisons with the L05 study. Furthermore, no *i*-band transformation comparisons can be made with any previous study since these transformations require *I_c*-band photometry which are not available for the LVL sample of galaxies.

Visual inspection of the previous transformation relationships with LVL galaxy colours overplotted (not shown for brevity) reveals similar results to those seen in Fig. 4. The LVL galaxy colours show large scatter around the previous transformation relationships and/or

Table 3. The *UBVR_c*-to-*ugri* transformation equations and coefficients for galaxies. The last column lists the rms scatter of the LVL galaxy colours around the least χ^2 fit for each transformation.

SDSS transformations		
Colour	Colour transformation	rms (mag)
$u - V$	$= (2.05 \pm 0.12)(B - V) + (0.10 \pm 0.06)$	0.06
$g - V$	$= (0.70 \pm 0.06)(B - V) + (-0.17 \pm 0.03)$	0.05
$r - B$	$= (-1.42 \pm 0.08)(B - V) + (0.01 \pm 0.04)$	0.06
$i - V$	$= (-2.29 \pm 0.23)(V - R) + (0.48 \pm 0.09)$	0.06

there exist significant deviations between the LVL best fits and those derived in previous studies.

To quantify the accuracy of previous transformations on galaxy colours, we calculate the rms scatter of the LVL galaxy colours around the previously published best-fitting line and ΔM_{med} values. The results are not graphically shown for brevity but yield similar results to the bottom panel of Fig. 2. All of the g -band and only one of the r -band transformations derived from previous studies yield low rms scatter and ΔM_{med} values (<0.1 mag). However, all of the u - and most of the r -band transformations show relatively high rms scatter ($0.1 < \text{rms} < 0.2$) and ΔM_{med} values ($0.1 < \Delta M_{\text{med}} < 0.3$). For every transformation of previous studies, there exists an LVL transformation with a lower rms scatter and ΔM_{med} value in every available bandpass.

4.2.3 Observed colour–colour trends

Due to the availability of only three transformed $ugri$ filters, we examine only one observed colour–colour trend which is not shown for brevity: $(g - r)_0$ versus $(u - r)_0$. We find similar results to those seen in Fig. 6 where the Jester et al. (2005), Jordi et al. (2006), and Blanton & Roweis (2007) transformations show similar slopes to the observed colour–colour trends, but the transformed colours of both Jordi et al. (2006) and Blanton & Roweis (2007) show a noticeable offset. Furthermore, the transformed colours of Jester et al. (2005) show an offset in both colours which are similar to the observed colour–colour relationship slope which indicates a systematic colour offset. Although we do not show this colour–colour figure, we have provided the median colour differences in Table 4.

The LVL galaxy transformations show good agreement with the observed colour–colour trends and show no systematic colour differences in Table 4. In addition, the LVL transformations consistently show smaller colour differences when compared to previous transformations. These results suggest that the LVL galaxy transformations more accurately describe the SDSS–Johnson–Cousins colour relationships for galaxies.

Table 4. The median colour differences between the $UBVR_c$ -to- $ugri$ transformed and observed colours for the LVL galaxy transformations and those derived in previous transformations.

Median colour differences		
Colour	Study	Δcolour (mag)
$(u - g)_0$	Jester et al. (2005)	−0.22
	Jordi et al. (2006)	−0.08
	Blanton & Roweis (2007)	−0.12
	LVL	0.01
$(u - r)_0$	Jester et al. (2005)	−0.34
	Jordi et al. (2006)	−0.04
	Blanton & Roweis (2007)	0.07
	LVL	−0.01
$(u - i)_0$	LVL	0.09
$(g - r)_0$	Jester et al. (2005)	−0.10
	Jordi et al. (2006)	0.01
	Blanton & Roweis (2007)	0.15
	LVL	0.01
$(g - i)_0$	LVL	0.03
$(r - i)_0$	LVL	0.04

4.3 Summary

We have derived empirical colour transformations for galaxies between the SDSS $ugri$ and Johnson–Cousins $UBVR_c$ photometric systems. We utilize the LVL nearby galaxy sample which consists of normal, non-starbursting galaxies. The data are taken from the LVL global optical photometry study of Cook et al. (2014a) where the fluxes were measured within identical apertures across all optical bandpasses to ensure consistent photometric comparisons.

The LVL galaxy transformations are derived via an analysis of all possible colour transformation combinations. The accuracy of each transformation is quantified via the rms scatter around the least χ^2 fit and the median absolute difference between the resulting transformed and observed magnitudes (ΔM_{med}).

We also compared our results to those of previous SDSS transformations derived from standard calibration stars (Jester et al. 2005; L05; Jordi et al. 2006) and model-based galaxy templates (Blanton & Roweis 2007). The rms scatter of LVL galaxy colours around each of the previously published transformations was calculated in addition to the resulting ΔM_{med} value. The observed galaxy colours show large scatter and/or significant offsets for most of the previous colour–colour relationships. Although *some* of the previous transformations yielded reasonable rms scatter and ΔM_{med} values in *some* filters, there are other filters (i.e. U and u band) where no previous transformation showed reasonable rms scatter and ΔM_{med} values (<0.15 mag). In addition, for each filter there exist multiple LVL transformations with lower rms scatter and ΔM_{med} values compared to the best stellar and model-based galaxy transformations.

A secondary check on the accuracy of both the LVL and previous transformations was performed by propagating the transformed magnitudes into colours and comparing them to observed colour–colour trends. We found that all previous transformations showed significant colour offsets (>0.1 mag) in more than one colour. In general, the model-based galaxy transformations of Blanton & Roweis (2007) showed smaller median colour differences compared to the stellar transformations, but the LVL transformations consistently showed either the smallest, or similar to the smallest, median colour difference in all colours. These results suggest that neither the stellar nor the model-based galaxy transformations can accurately describe all colour transformations for observed galaxies when compared to the empirically derived LVL-based galaxy transformations.

ACKNOWLEDGEMENTS

The authors thank the anonymous referee for helpful comments. Support for this work, part of the *Spitzer* Space Telescope Legacy Science Program, was provided by National Aeronautics and Space Administration (NASA) through contract 1336000 issued by the Jet Propulsion Laboratory, California Institute of Technology under NASA contract 1407. This research has made use of the NASA/IPAC Extragalactic Database, which is operated by JPL/Caltech, under contract with NASA. IRAF is distributed by the National Optical Astronomy Observatory, which is operated by the Association of Universities for Research in Astronomy (AURA) under cooperative agreement with the National Science Foundation.

Funding for the SDSS and SDSS-II has been provided by the Alfred P. Sloan Foundation, the Participating Institutions, the National Science Foundation, the U.S. Department of Energy, the National Aeronautics and Space Administration, the Japanese

Monbukagakusho, the Max Planck Society, and the Higher Education Funding Council for England. The SDSS Web Site is <http://www.sdss.org/>.

The SDSS is managed by the Astrophysical Research Consortium for the Participating Institutions. The Participating Institutions are the American Museum of Natural History, Astrophysical Institute Potsdam, University of Basel, University of Cambridge, Case Western Reserve University, University of Chicago, Drexel University, Fermilab, the Institute for Advanced Study, the Japan Participation Group, Johns Hopkins University, the Joint Institute for Nuclear Astrophysics, the Kavli Institute for Particle Astrophysics and Cosmology, the Korean Scientist Group, the Chinese Academy of Sciences (LAMOST), Los Alamos National Laboratory, the Max-Planck-Institute for Astronomy (MPIA), the Max-Planck-Institute for Astrophysics (MPA), New Mexico State University, Ohio State University, University of Pittsburgh, University of Portsmouth, Princeton University, the United States Naval Observatory, and the University of Washington.

REFERENCES

- Abazajian K. N. et al., 2009, *ApJS*, 182, 543
 Bertin E., Mellier Y., Radovich M., Missonnier G., Didelon P., Morin B., 2002, in Bohlender D. A., Durand D., Handley T. H., eds, *ASP Conf. Ser. Vol. 281, Astronomical Data Analysis Software and Systems XI*. Astron. Soc. Pac., San Francisco, p. 228
 Blanton M. R., Roweis S., 2007, *AJ*, 133, 734
 Blanton M. R. et al., 2003, *ApJ*, 594, 186
 Bruzual G., Charlot S., 2003, *MNRAS*, 344, 1000
 Cook D. O. et al., 2014a, *MNRAS*, 445, 881
 Cook D. O. et al., 2014b, *MNRAS*, 445, 899
 Cousins A. W. J., 1976, *Mon. Notes Astron. Soc. South. Afr.*, 35, 70
 Dalcanton J. J. et al., 2009, *ApJS*, 183, 67
 Dale D. A. et al., 2009, *ApJ*, 703, 517
 de Vaucouleurs G., de Vaucouleurs A., Corwin H. G., Jr, Buta R. J., Paturel G., Fouqué P., 1991, *Third Reference Catalogue of Bright Galaxies. Volume I: Explanations and references. Volume II: Data for galaxies between 0^h and 12^h. Volume III: Data for galaxies between 12^h and 24^h*
 Jester S. et al., 2005, *AJ*, 130, 873
 Johnson H. L., Morgan W. W., 1953, *ApJ*, 117, 313
 Jordi K., Grebel E. K., Ammon K., 2006, *A&A*, 460, 339
 Karaali S., Bilir S., Tunçel S., 2005, *PASA*, 22, 24
 Kennicutt R. C., Jr, Funes Lee J. C., José G. S. J., Sakai S., Akiyama S., 2008, *ApJS*, 178, 247
 Landolt A. U., 1992, *AJ*, 104, 340
 Lee J. C. et al., 2011, *ApJS*, 192, 6
 Murphy E. J. et al., 2011, *ApJ*, 737, 67
 Rodgers C. T., Canterna R., Smith J. A., Pierce M. J., Tucker D. L., 2006, *AJ*, 132, 989
 Smith J. A. et al., 2002, *AJ*, 123, 2121
 Stetson P. B., 2000, *PASP*, 112, 925
 Thuan T. X., Gunn J. E., 1976, *PASP*, 88, 543
 West A. A., Walkowicz L. M., Hawley S. L., 2005, *PASP*, 117, 706
 York D. G. et al., 2000, *AJ*, 120, 1579

This paper has been typeset from a $\text{\TeX}/\text{\LaTeX}$ file prepared by the author.